ACS OMEGA

http://pubs.acs.org/journal/acsodf

Article

Innovative Applications of Red Mud: Converting an Environmental Challenge to a Drilling Asset

Reem AlBoraikan,* Badr Bageri, and Theis I. Solling

Cite This: *ACS Omega* 2023, 8, 614−625

Read Online

ACCESS | Metrics & More | Article Recommendations

ABSTRACT: Red mud is generated from alumina production through bauxite digestion with caustic soda. Ma'aden aluminum production estimated the abundance in a million tons as 2.65:1:2 for bauxite, alumina, and red mud, respectively. The real challenge when it comes to red mud pertains to storage capacity; many solutions have been put forward in different industries, and in this study, the utilization of the red mud waste material is presented as a potential weighting material that could be incorporated into the design of drilling fluid systems. This study provides an assessment of the utilization of red mud as a drilling fluid, and it provides directions for the use of red mud in drilling mud systems as a filtration agent and as a finely divided solid used as a weighting material to increase the density of a given drilling fluid system. This study investigates the viability of red mud as an effective additive to drilling fluid and its effect on rheology and filtration. Different techniques are employed in red mud characterization and performance evaluation. The study assesses red mud as an inert solid in a drilling fluid system by investigating the drilling fluid rheology, apparent viscosity (AV), plastic viscosity (PV), and yield point (YP) before and after hot rolling at 150 °F, in addition to filtration properties under low-pressure, low-temperature and higher-pressure, higher-temperature conditions (at 150 °F and a differential pressure of 250 psi). Also, the study highlights the red mud solid characterization, material preparation, and acid dissolution at 150 °F. This study attempts to view the red mud situation from a practical application angle (primarily in the oil and gas industry). Test results show stable drilling mud fluid properties when utilizing red mud solid additives as weighting agents. The drilling mud exhibits relatively low plastic viscosity, gel strength, excellent sag behavior, and reasonable filtration control, even under HPHT conditions in aqueous-based fluids. The material dissolves in acid. Accordingly, red mud provides a viable option for weighting agents and filtration control.

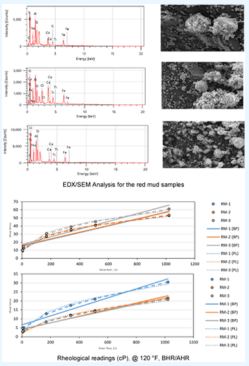

1. INTRODUCTION

Over the years, researchers worldwide have extensively developed various economical ways for red mud utilization in agriculture, construction, sewage treatment, waste gas treatment, etc.[1] Exploring other areas for red mud utilization in the oil and gas industry would be a new area of research. Over the past 10 years, there have been many publications related to red mud utilization in the fields of construction and agriculture, in the chemical industry, and for the extraction of valuable elements.[1] The flowchart below shows the purification of bauxite to produce aluminum. Bauxite goes through a digestion process with caustic soda, as shown in Figure 1. The aluminum production in the eastern region yields about 4 million tons of waste material in the form of the so-called red mud or bauxite residue. This is a real challenge when it comes to storage capacity. The waste material is basic (pH > 12) and rich in a range of different nontoxic metals, so it has the potential to be reused in a range of various applications. With the high demand for energy around the globe and the global increase in technological competitiveness, the upsurge and the need to find solutions for waste prevention that could be applicable in the oil and gas sector have become a priority for oil companies. As such, providing solutions will prevent/minimize waste. The direction provided in this study targets additives that are used in drilling fluids to obtain specific properties. The focus is on the application of red mud in drilling where it has potential because of its mineralogical composition and characteristics.

In the past few years, there has been significant interest in research and development within the oil and gas sector on evaluating different waste materials as additives, specifically for water-based drilling fluids. Studies were focused on the improvement of the rheological and filtration properties in particular.[2−7] Since 1922, many weighting agents such as barite, hematite, Micromax, and ilmenite have been used to increase the density of drilling fluids. However, the use of a specific weighting agent depends on the specific drilling circumstances.[8−13] Weighting agents are used in drilling fluids to adjust the density. There are two approaches to achieve the proper density: solid loading and the addition of concentrated brines. Selecting the proper weighting agent becomes crucial, especially for higher-

Received: September 5, 2022
Accepted: December 6, 2022
Published: December 26, 2022

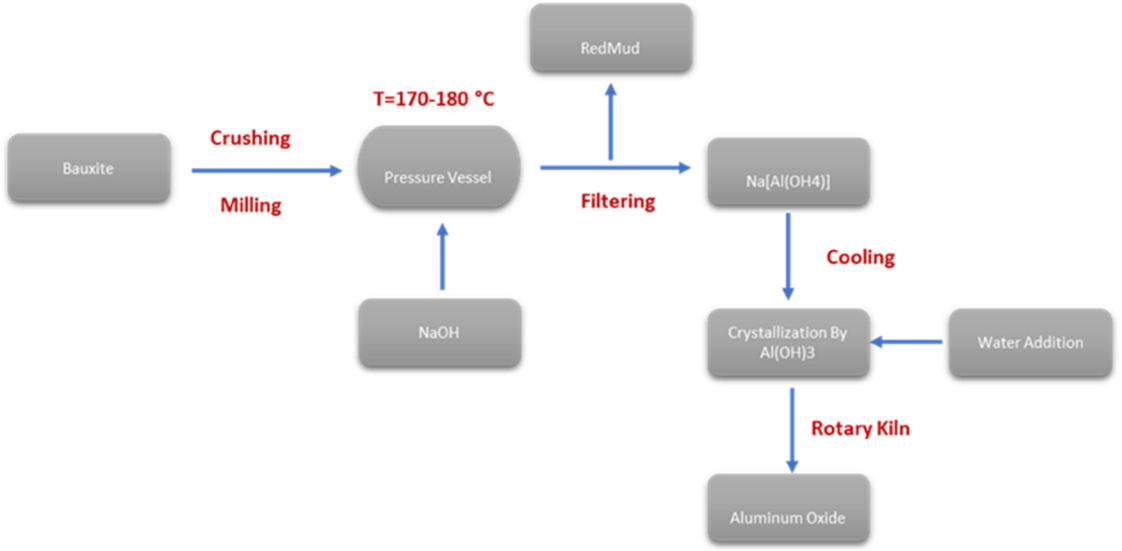

Figure 1. Schematic showing the digestion process of Bauxite.

Figure 2. Collected red mud samples.

density drilling fluids, to achieve an appropriate rheological profile with low plastic viscosity and friction.[11] Also, the weighting agent cannot exhibit a tendency to settle.[11,14] Moreover, the hardness of the solid particles that constitute the weighing agent plays a considerable role; to avoid formation damage and rheological instabilities, they cannot be too hard. At the same time, the size of the particles matters; to prevent abrasion, the number of coarse particles must be kept at a minimum. Finally, the material has to be readily available, cheap, and, last but not least, comply with local and global HSE regulations, including those related to sustainability aspects.[12]

Here, an assessment of the chemical and mineralogical characteristics provided directions for using red mud as an inert additive in drilling fluids. This study describes a new solid material that can be incorporated into a drilling fluid system as a weighting agent. The material is suitable for drilling fluids and offers significant advantages regarding rheology, filtration behaviors, and sag tendency. The density of bulk red mud is around 2.85 s.g. It is a light mineral with the usual reddish-brown color caused by the higher iron content.[15]

As a result of the low specific gravity of red mud, this study focused on its application as a low-density drilling fluid (LDDF). The present study will assess whether it fulfills the requirements of being available in sufficient volumes, is competitively priced, and provides better functionality as a drilling fluid. If these conditions are met, red mud will be a perfect example of a material where trash is turned into treasure. The red mud characteristics and performance established in this study present a waste management opportunity for the complex challenge faced by the manufacturer in terms of storage capacity as well as an opportunity to utilize the material in the drilling operation, as a chemical additive in conventional (LDDF) water-based systems that contributes to the control of drilling fluid properties.

$$Al_2O_3{\cdot}xH_2O + 2NaOH \rightarrow 2NaAlO_2 + (x+1)H_2O$$

2. RED MUD COLLECTION AND TREATMENT

The seemingly endless red mud flats at Ras Al Kheir result from the production of aluminum from the ore mined in Qassim. The process yields more than 50% waste, with an annual output of around 2.65 million tons, which is more than enough for a wide range of applications, and drilling mud is only one example. A

https://doi.org/10.1021/acsomega.2c05755
ACS Omega 2023, 8, 614−625

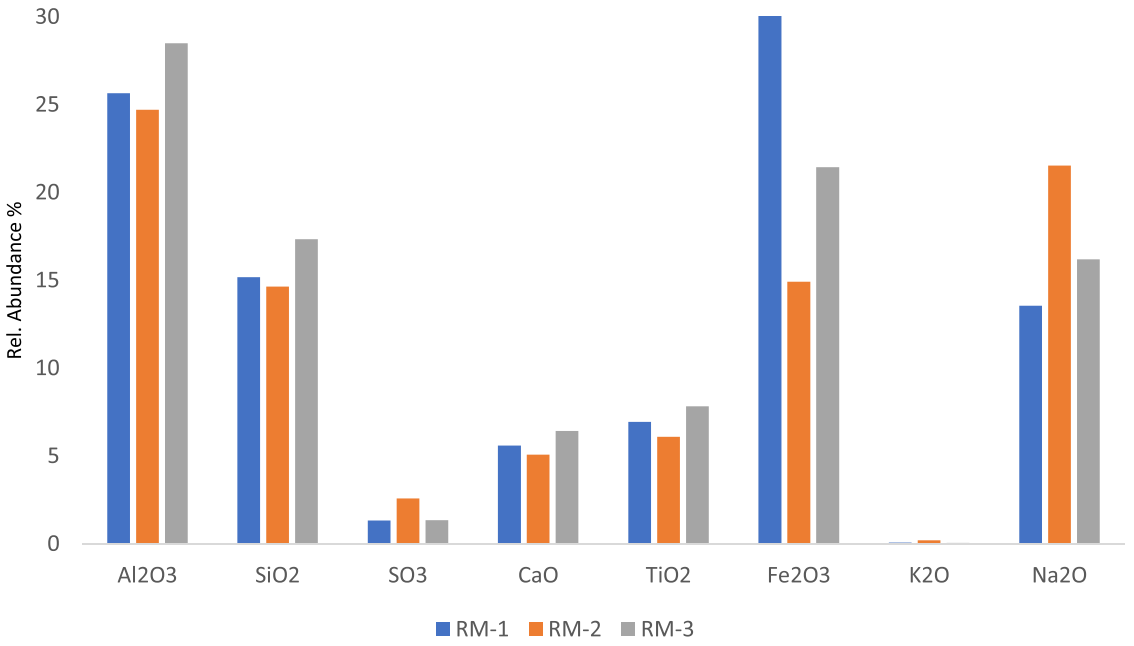

Figure 3. Oxide composition of the red mud determined by XRF.

sampling campaign was conducted at Ras Al Kheir, where three different samples, red mud-1 (RM-1), red mud-2 (RM-2), and red mud-3 (RM-3) (Figure 2), were collected from separate locations. The samples varied in their moisture contents and particle sizes (large, medium, and small). The collected samples were treated by (1) drying for a maximum of 48 h under 212 °F and (2) grinding using rotating mechanical milling at 400 rpm. Then, a sieving process also has to be implemented for the dry material to match the global standard of the weighting agent. The primary challenge is to avoid the loss of the red mud additive while the drilling mud goes through solid removal equipment, i.e., shale shaker, mud cleaner, desander, desilter, and centrifuge.[16] Therefore, the resulting ground/dried red mud powder was sieved through a 100 micron mesh. After treatment, the samples were characterized with respect to their densities, solid characteristics, and fluid properties.

3. RESULTS AND DISCUSSION

3.1. Red Mud Evaluation. *3.1.1. Solid Characteristics.* The characterization of the solids, which includes the determination of the mineralogical composition, was performed using different techniques. Starting with energy-dispersive X-ray fluorescence (XRF) analysis (JSX-1000S X-ray fluorescence spectrometer), the X-ray tube was operated at 30 KeV voltage and 0.030 mA current to identify the elemental composition. The weighted powder samples were placed in the appropriate holder with a transparent cover. Before analysis, the powder samples required proper mounting for an accurate diffraction measurement. Then, the element peaks were automatically recorded using the solution application provided with XRF. Furthermore, energy-dispersive X-ray/scanning electron microscopy (EDX-SEM) interpretation was performed using a Joel 7000 desktop scanning electron microscope. After placing the powdered samples in the proper holder, the samples were coated with a 2 nm gold layer; then, both surface morphology and live map EDX analysis were performed to view the elemental distribution in real time.

The elemental and oxide compositions of the red-mud-treated samples were determined by (XRF) for the three samples. The samples are mostly consistent. The data showed high concertation ranges for iron (20−40%), aluminum (19−22%), sodium (17−20%), and silica (11−12%). The oxide analyses reveal that the concentration of aluminum oxide (Al_2O_3) in the red mud ranges between 25 and 28%, iron oxide (Fe_2O_3) between 14 and 30%, silicon dioxide (SiO_2) between 14 and 17%, and sodium oxide (Na_2O) between 13 and 21%, as shown in Figure 3.

The EDX measurements agree with the XRF data (Table 1 and Figure 4), with the predominance of iron, sodium, aluminum, and silica. Moreover, SEM imaging was performed to generate a high-resolution image to investigate the particle shape with high-magnification images of the surface topography for the three samples. The imaging showed that the samples consist of a heterogeneous particle distribution with regard to shape, with predominantly very fine particles (Figure 5).

Table 1. Relative EDX Elemental Composition of Red Mud

name	C	O	Na	Al	Si	Ca	Ti	Fe
RM-1	6	38	7	12	6	7	5	18
RM-2	8	30	7	9	4	10	6	20
RM-3	6	43	5	19	5	5	5	11
avg.	7	37	7	13	5	7	6	17

3.1.2. Particles Size Distribution Analysis. The particle size distribution (PSD) of the treated red mud additive was determined using a Malvern Mastersizer 2000 wet particle size analyzer. Laser diffraction utilizes the intensity of the laser beam that moves through a dispersed particulate sample. The distribution (D) is expressed in three different values: D (0.1) represents 10% of the particles smaller than the captured data size, D (0.5) indicates the median particle size distribution, and D (0.9) means that 90% of the total particles are smaller than the captured data size.

Figure 6 shows the PSD range for the three treated red mud weighting additives. The D (0.5) sample distribution ranged

https://doi.org/10.1021/acsomega.2c05755
ACS Omega 2023, 8, 614−625

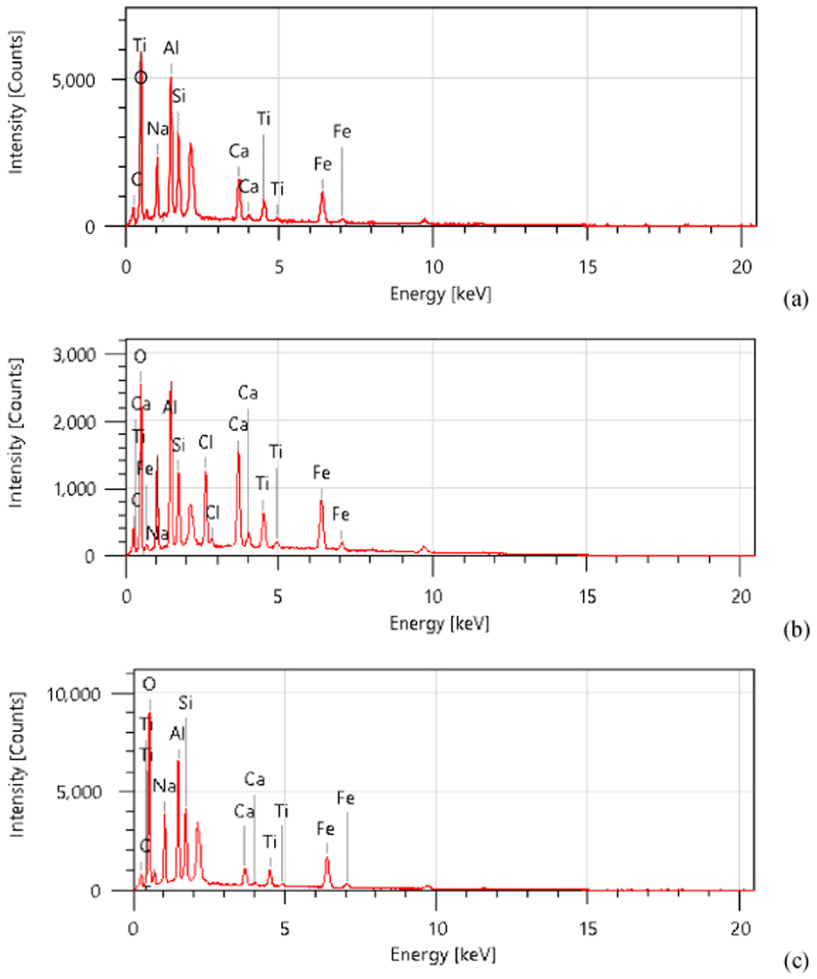

Figure 4. EDX analysis of the red mud samples: (a) RM-1, (b) RM-2, and (c) RM-3.

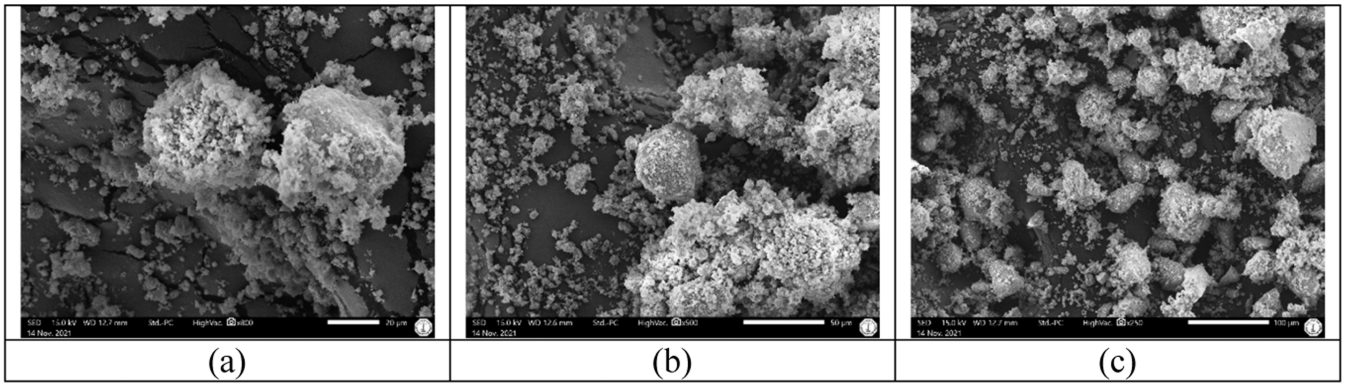

Figure 5. SEM images of the red mud samples: (a) RM-1, (b) RM-2, and (c) RM-3.

from 1.4 to 24.8 μm, and the D (0.9) sample distribution ranged from 26−55 μm. The median particle size distribution D (0.5) and the size of the fine and large particles in terms of D (0.1) and D (0.9) are shown in Table 2. In this study, the impact of red mud addition on the invasion of drilling mud into the porous media is explained in the filtration evaluation section.

3.2. Drilling Fluid Preparation. Table 3 presents the composition of the drilling mud formulations in this study. The drilling fluid samples were prepared using a fixed concentration of red mud at 80 lb./bbl. as a weighting agent. This formulation was selected with reference to past water-based drilling fluids that had been weighted using calcite as a weighting agent[16,17] at similar concentrations. The unweighted spud mud was prepared using x-polymer and potato starch to enhance the rheological behavior, solid suspension, and filtration control of the drilling fluid.

The properties, density, and pH of mud were identified for the red mud formulations using an atmospheric mud balance and a pH meter. The samples were conditioned in a dynamic rotating oven for 16 h at 150 °F to acquire the fluid properties related to the rheological and filtration behaviors after hot rolling (AHR).

https://doi.org/10.1021/acsomega.2c05755
ACS Omega 2023, 8, 614−625

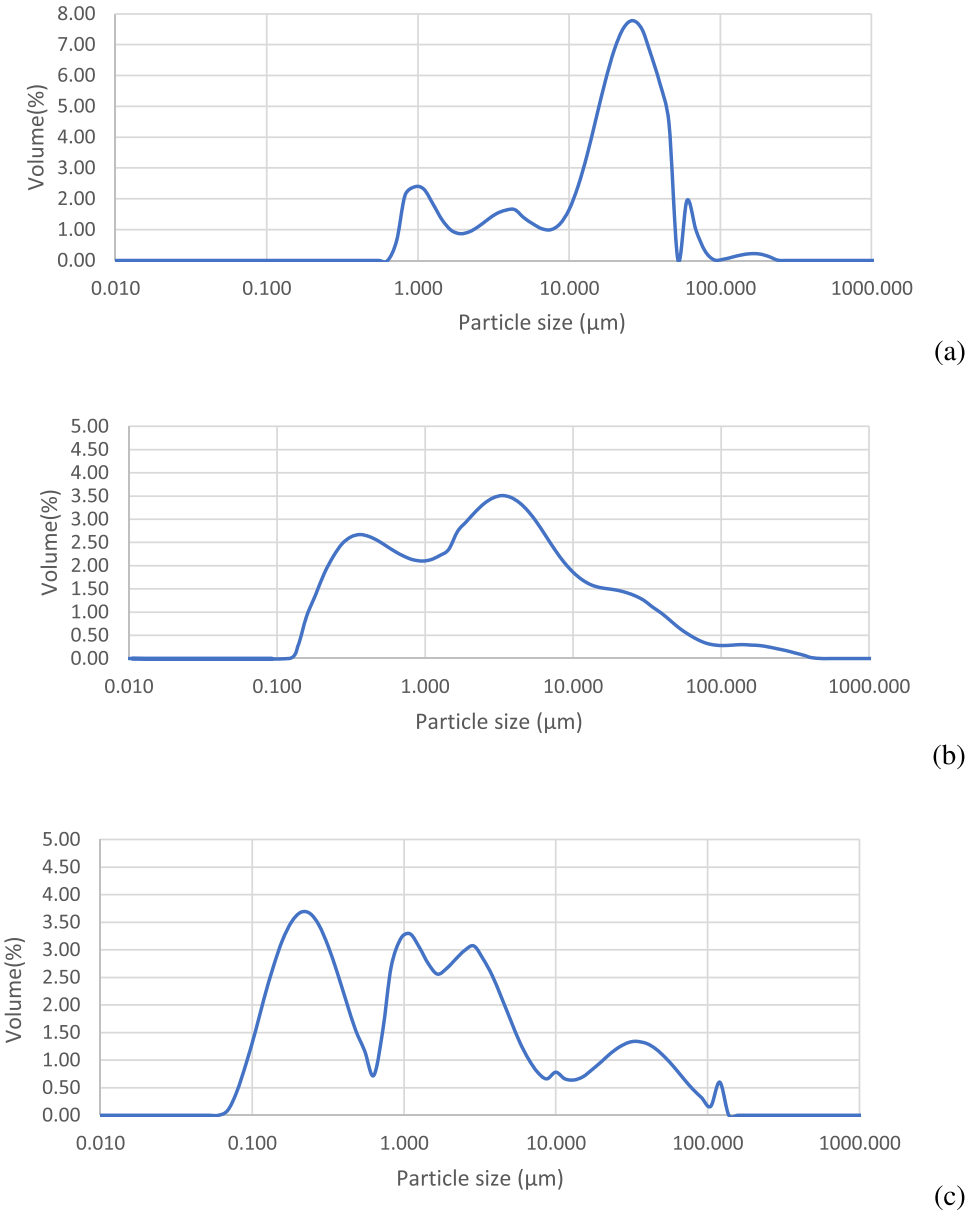

Figure 6. PSD of the red mud samples: (a) RM-1, (b) RM-2, and (c) RM-3.

Table 2. Particle Size Distribution Characteristics of Red Mud Samples

sample	D (0.1), μm	D (0.5), μm	D (0.9), μm
RM-1	1.55	24.89	55.17
RM-2	0.33	3.042	30.17
RM-3	0.18	1.43	26.28

Table 3. Drilling Fluid Formulation

component	red mud	mixing time (min)
water	0.88 bbl.	
defoamer	0.08 Ib	1
XC-polymer	1.5 Ib	20
starch	6 Ib	20
KCl	80 Ib	10
KOH	0.3 Ib	1
sodium sulfide	0.25 Ib	1
red mud	80 Ib	15

The rheological properties are determined by measurement of the apparent viscosity (AV), plastic viscosity (PV), and yield point (YP) using an OFITE viscometer Model 900 viscometer at 120 °F. The below equations were used to derive the PV and YP measurements. The capacity of the drilling fluid to build up the gelling behavior for the solid lifting capacity is measured for the red mud formulations by measuring the gel strength at 10 s and 10 min under static conditions. The gel strength dial reading was estimated directly at the lowest shear rate (3 rpm).

$$\text{PV} = \text{reading } \varnothing_{600} - \text{reading } \varnothing_{300}\#$$

$$\text{YP} = \text{reading } \varnothing_{300} - \text{PV}\#$$

$$\text{AV} = \frac{\text{reading } \varnothing_{600}}{2}\#$$

3.3. Drilling Fluid Evaluation. The water-based drilling fluid with the composition presented in Table 3 was selected and prepared using a fixed concentration of the red mud at 80 lb./

https://doi.org/10.1021/acsomega.2c05755
ACS Omega 2023, 8, 614−625

Table 4. OFITE Viscometer, Rheological Readings @ 120 °F

BHR				AHR			
RPM	RM-1	RM-2	RM-3	RPM	RM-1	RM-2	RM-3
600	52.9	53.6	61.3	600	30.5	21.6	20.8
300	41.1	40.6	45.3	300	21	14.6	14.1
200	34.9	35.5	38.8	200	17.5	12.1	11.8
100	27.0	27.4	30.7	100	12.8	8.3	8.3
6	12.1	12.1	14.7	6	5	3	3.5
3	9.0	10.6	10.2	3	4.7	2.8	3
AP, cP	26.5	26.8	30.7	AP, cP	15.3	10.8	10.4
PV, cP	11.8	13.0	16.0	PV, cP	9.5	7.0	6.7
YP, lb./100 ft^2	29.3	27.6	29.3	YP, lb./100 ft^2	11.5	7.6	7.4
YP/PV	2.5	2.1	1.8	YP/PV	1.2	1.1	1.1
Gel 10 s lb./100 ft^2	10.0	9.0	10.0	Gel 10 s lb./100 ft^2	3.0	3.0	3.0
Gel 10 min lb./100 ft^2	6.0	8.5	6.0	Gel 10 min lb./100 ft^2	5.0	4.0	4.0

bbl. The fluid type, concentration, and investigation results were benchmarked against a similar formulation based on calcite 16 utilizing the same formulation with 80 lb./bbl. calcite. The red mud additive was used as a weighting agent, and the prepared fluid was assessed based on its density, pH, rheological behavior, filtration properties, and acid solubility. The low density of the treated red mud additive governs the targeted tested formulations for the low-density drilling fluid (LDDF) application. The samples were prepared, and the density for the red mud drilling was around 10 pounds per gallon (ppg). Using an equal dosage of 80 Ib/bbl., the red mud and calcite-weighted drilling fluid exhibit similar densities,[16,17] which was expected due to the similarity in the densities of the materials. Moreover, the pH of the red mud samples is around 11. The measured pH was within the normal range for drilling fluids.

Experimental data show that the rheological properties before hot rolling (BHR) and after hot rolling (AHR), starting from the rheology readings at six different speeds (600, 300, 200, 100, 6, and 3 rpm), show relatively similar rheological behaviors of the three samples (RM-1, R M-2, and RM-3), as shown in Table 4. Moreover, drilling fluid viscosity models such as the Bingham plastic, power law, and Herschel−Bulkley models, were implemented to fit the shear rate data vs. the shear stress. Among these models, the Herschel−Bulkley model showed the best fit to describe the rheological behavior of the prepared red mud (see Table 5 and Figures 7 and 8).

Table 5. Rheological Parameters Described by the Herschel−Bulkley Model

		Herschel−Bulkley				
		K	*n*	YS	RMSE	*R*-square
BHR	RM-1	2.69	0.418	4.26	0.614	0.9992
	RM-2	2.17	0.445	6.06	0.277	0.9998
	RM-3	2.05	0.472	7.14	1.26	0.9974
AHR	RM-1	0.420	0.601	3.47	0.212	0.9997
	RM-2	0.262	0.623	1.98	0.176	0.9996
	RM-3	0.234	0.630	2.41	0.167	0.9996

The measurements of AV and PV presented here were obtained to evaluate the fluid resistance to flow due to the mechanical friction generated from solid, solid/fluid, and fluid interactions.[18] Figure 9 demonstrates the AV for the red mud samples before and after hot rolling. The AV readings for the red mud samples BHR are in the range of 26−31 cP. This result indicates that the red mud samples behave similarly to calcite mud in a previous study.[16] However, the result variation for red mud samples can be correlated to differences in the PSD analysis of the red mud, as shown in Table 2. In addition, there was a reduction in the viscosity for the red mud samples AHR, and the AV decreased to a lower range (10−15 cP). Interestingly, results of the three samples yield relatively close viscosities, BHR and AHR, which indicates that the red mud treatment has a minor impact on the rheological properties, as shown in the AV results. Moreover, PV measurements for the three samples are similar, as shown in Figure 10. The samples under study, BHR and AHR, yielded values in the ranges of 12−16 and 7−10 cP, respectively. The yield point (YP) for the present samples BHR range from 27 to 29 (lb./100 ft^2), as shown in Figure 10. This result confirms that the red mud samples have rheological properties similar (and favorable) to those of calcite mud. Furthermore, the yield point for the AHR samples was in the range of 7−11.5 (lb./100 ft^2).

The carrying capacity index (YP/PV) was also calculated. The BHR samples yielded carrying capacities higher than 1 (2.5, 2.1, and 1.8, respectively). This indicates that the red mud samples are able to carry solids quite efficiently. However, the YP/PV index is reduced due to heating, as indicated by the AHR results. The YP/PV indices were 1.2, 1.1, and 1.1, respectively. As can be seen from Figure 11, all samples yielded an index higher than 1. This shows that the drilling fluids provide an excellent solid suspension and low settling velocity. Lastly, the gel strengths (GSs) were obtained directly from the dial reading at 3 rpm after the static gelling time of 10 s and 10 min. Figure 12 shows that the gel strengths for the BHR samples are in the range of 9−10/6−8.5 (lb./100 ft^2) for the 10 s/10 min readings, respectively, which are close to the values of weighted calcite mud at 13/14 (lb./100 ft^2). Also, the AHR gel strength readings were aligned with unweighted polymer mud behavior; the samples display 3 lb./100 ft^2 for a 10 s reading and 4−5 lb./100 ft^2 for a 10 min reading. Overall, the result demonstrates, as shown in Table 4, a comparatively similar rheological behavior for RM-1, RM-2, and RM-3 BHR. On the other hand, RM-1 exhibited higher AHR rheology readings compared with RM-2 and RM-3. The variations in the red mud rheology readings due to the variation in red mud PSD analysis as the PSD analysis for RM-1 demonstrates a higher *D* (0.1) *D* (0.5) *D* (0.9) particle size distribution compared with RM-2 and RM-3, as shown in Table 2.

3.4. Filtration Properties of Drilling Fluids. The fluid filtration properties were acquired after hot rolling (AHR) to mimic the real conditions for the drilled section. The samples

https://doi.org/10.1021/acsomega.2c05755
ACS Omega 2023, 8, 614−625

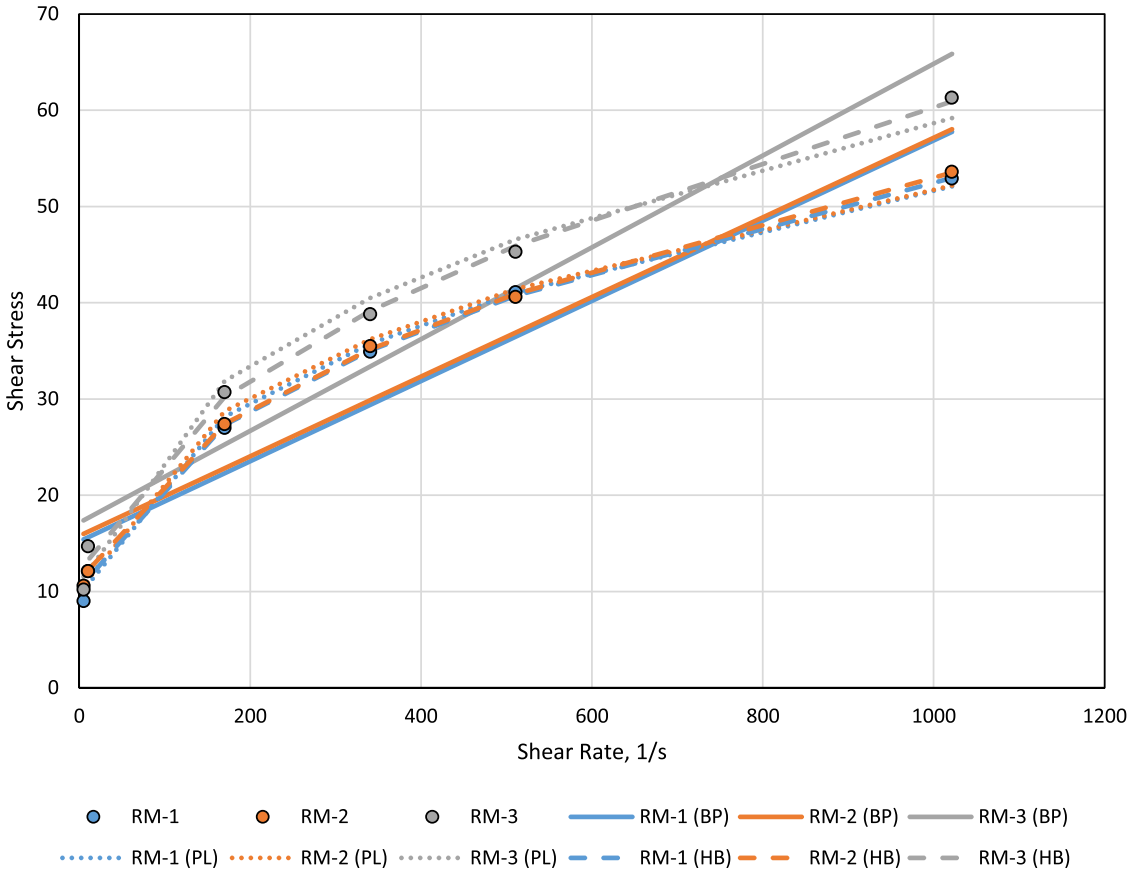

Figure 7. Rheological Readings (cP), @ 120 °F, BHR.

were conditioned in a dynamic rotating oven for 16 h at 150 °F. Then, API experimental tests were run using a standard Multiple Unit Filter Press, at low pressure, low temperature with 100 psi working pressure and at high pressure, high temperature with 250 psi differential pressure (DP). Both low-pressure low-temperature (LPLT) and high-pressure high-temperature (HPHT) filtration were conducted through filter paper and a ceramic disk with 40 μm pore size consecutively as a filter medium for LPLT and HPHT evaluation.

In this study, the fluids based on calcite were the benchmark samples, and they were used as the reference for comparison purposes.[16,17] During the LPLT/HPHT filtration process, the fluid loss "filtrate" was collected over 30 min in a graduated cylinder. The total filtration volume was captured directly at the end of the fluid loss test. Based on the comparisons with the calcite-based mud, the results were extracted.

3.4.1. Fluid Loss Test (LPLT). The results for the three red mud samples (RM-1, RM-2, and RM-3) indicate that the filtration of red mud drilling fluids is behaving acceptably and closely as the filtrate for red mud samples ranges from 5.2 to 7.7 mL, as shown in Figure 13. Furthermore, 5.8 mL was the lowest fluid loss volume for RM-2 compared with the other red mud samples RM-1 and RM-3. The minor variation in performance is due to the dissimilarity in the PSD of samples, and the D (0.5) variation for the prepared samples, such as the filterability and compressibility of the filter cake, is highly affected by the particle size and concentration. The wider the area and the broader the distribution of the particles, the stronger the layered filter cake[19] (Figure 6 and Table 2). The nature of the filter cake will impact the wellbore stability and control the phenomenon of fluid invasion into the formation. A benchmark experiment was conducted using the same drilling fluid formulation with calcite as a weighting agent.[16] The results show a slightly higher LPLT filtration volume for the red mud drilling fluids than for calcite mud (4.5 mL). However, the red mud yields LPLT filtration performance within the accepted range if compared with many other recent additives.

In addition to the LPLT investigation, the red mud drilling fluid was subjected to high-pressure, high-temperature (HPHT) testing to assess the filter cake deposition over the filter medium.[20] The instantaneous filtration volume for the sample was obtained in this study. The drilling filtrate (spurt volume) that passes through the filter medium at the beginning of HPHT static filtration is associated with how fast the solid deposits over the ceramic medium, near zero filtrate volume, and this indicates how easy it is to control the fluid invasion into the reservoir.[21,22]

3.4.2. HPHT Fluid Loss (Ceramic Disk Size 40 μm). The HPHT filtration was performed using a ceramic disk with 40 μm pore space @ 150 °F and a differential pressure (DP) of 250 psi. As mentioned in the previous sections, the rheology readings and LPLT testing for the three samples were relatively comparable, and RM-2 exhibited better performance.Therefore, HPHT filtration was performed for RM-2. The variances LPLT in the behaviors of samples can be correlated to PSD as the scientific reason for variations in red mud performance. Therefore, HPHT filtration was performed for RM-2, and the red mud drilling fluids exhibited good filtration behavior (Figure 14). Figure 15 shows a total filtrate of 5.2 mL, including 2 mL spurt loss. The result indicates a fast filter cake deposition over the ceramic disk and allows fluid loss volume, as shown in Table 6 and Figure 14. Moreover, the red mud drilling fluid was tested with a 50 μm ceramic disk, and the behavior was similar. This

https://doi.org/10.1021/acsomega.2c05755
ACS Omega 2023, 8, 614−625

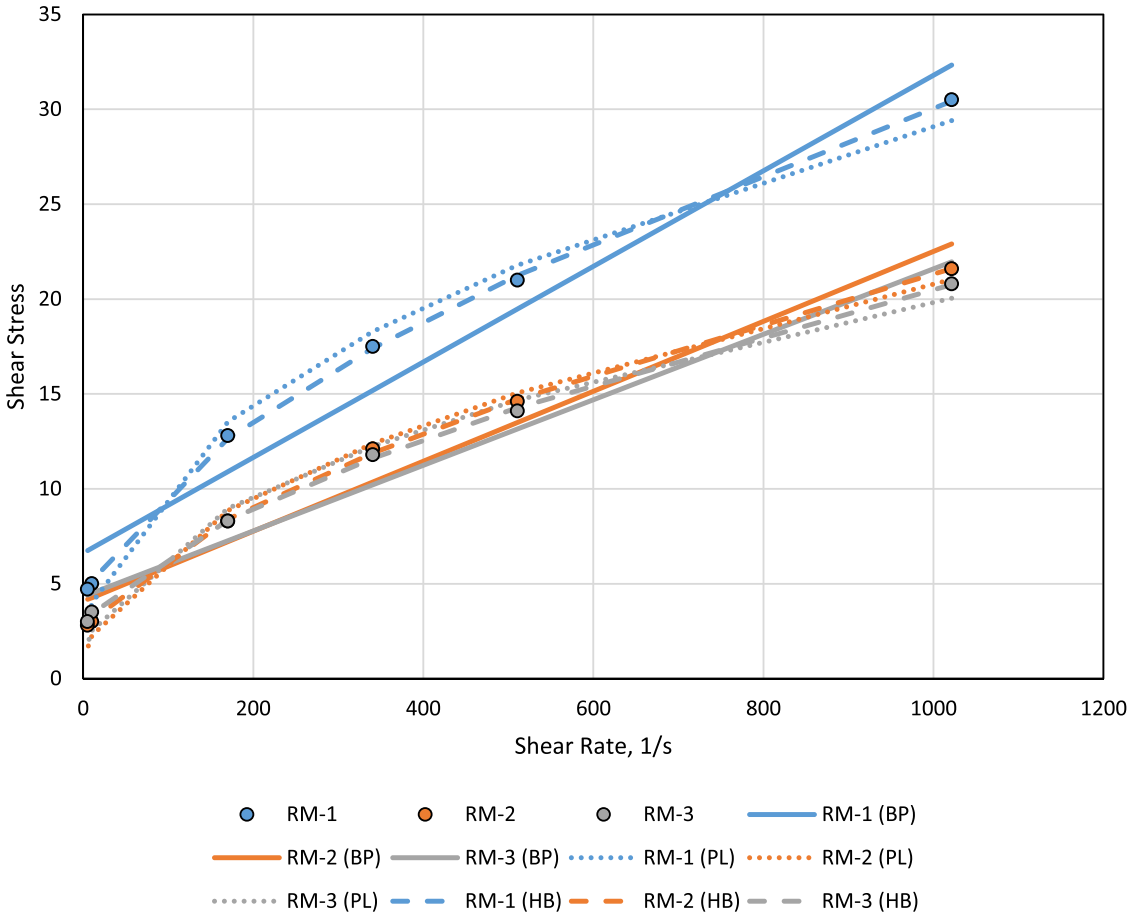

Figure 8. Rheological Readings (cP), @ 120 °F, AHR.

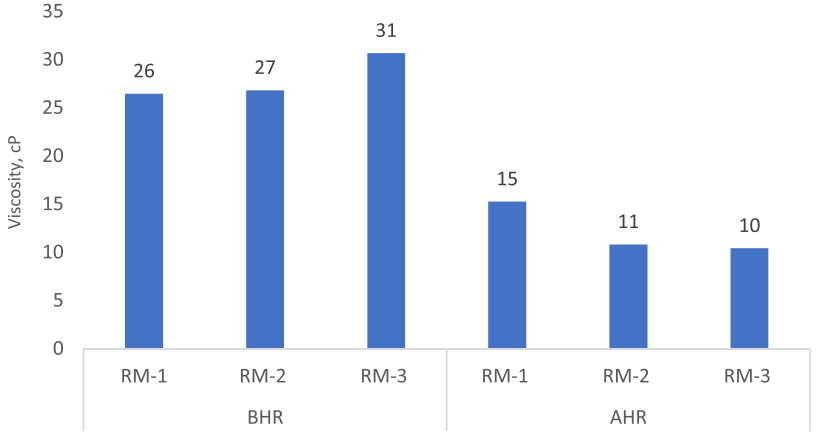

Figure 9. BHR/AHR apparent viscosity (AP), cP.

observation shows that the red mud-based fluid, when applied over a 50 μm ceramic disk, forms superior filter cakes compared with the calcite mud utilizing the same formulation. The filter cake thickness was 2.8 mm for calcite mud,[16] while the red mud showed 1.5 mm filter cake thickness, as shown in Table 6.

3.5. Red Mud Acid Dissolution. The solubility in 15% HCl of the bauxite powder ore from the red mud flats at Ras Al Kheir was evaluated. The samples were dissolved in hydrochloric acid to determine the optimum dissolution rate under specific conditions. The dissolution experiment was carried out in a conical flask using a heated magnetic stirrer in different time frames (2, 3, and 4 h). Table 7 shows the dissolution percentage with 15% HCl. Many factors affect the dissolution and the kinetic process, such as acid concentration, particle size, stirrer speed/agitation, and temperature, which require further investigation.[23] After 4 h, the red mud sample shows around 50% acid dissolution. Figure 16 demonstrates the residue as (wt) and the dissolution rate as (w/w%) in different time frames sequentially.

4. CONCLUSIONS

The experimental work was conducted in a laboratory to investigate the feasibility of using red mud as a drilling fluid additive. The results show that red mud (density 2.85 s.g.) can

https://doi.org/10.1021/acsomega.2c05755
ACS Omega 2023, 8, 614−625

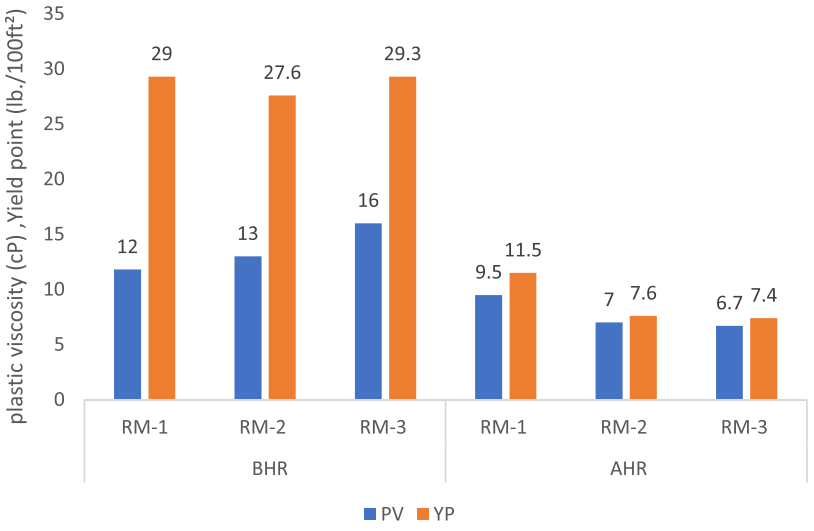

Figure 10. BHR/AHR plastic viscosity (PV), cP, and yield point (YP), lb./100 ft^2.

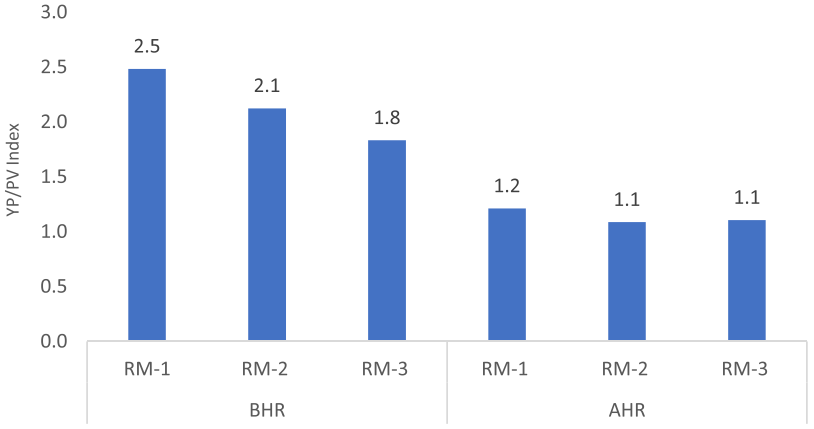

Figure 11. BHR/AHR cutting transportation index, YP/PV.

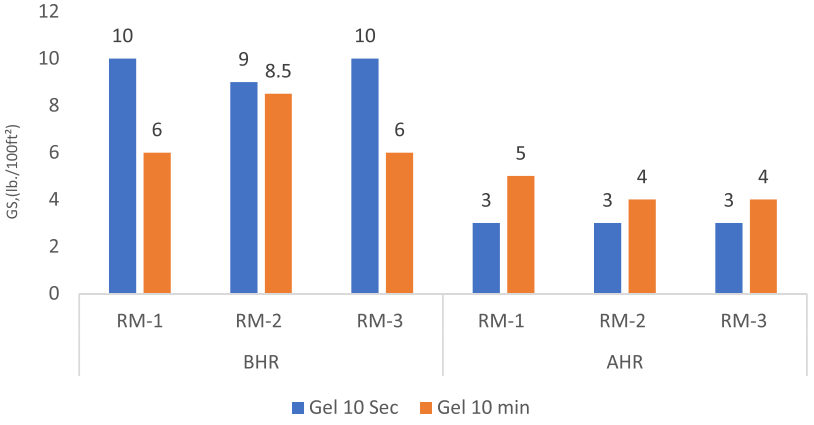

Figure 12. BHR/AHR gel strengths (lb./100 ft^2).

be used as a weighting agent in low-density drilling fluid applications. This was concluded based on the following main discoveries:

(1) The red mud drilling fluid exhibits rheological and filtration performance similar to those of calcite mud, a well-known base fluid.[16] The YP/PV ratio for the red mud samples ranged from 1.1 to 1.2 AHR. This measurement indicates the efficiency of red mud drilling fluids in the carrying capacity and hole cleaning ability.

(2) The red mud drilling fluid exhibited a higher ability to flow due to a slight reduction in AV and PV readings compared with calcite mud by 20−30%.

(3) The red mud drilling fluid demonstrated a higher 10 min gel strength reading than calcite mud, excellent sag behavior, and reasonable filtration control under LPLT and HPHT conditions in aqueous-based fluids.

https://doi.org/10.1021/acsomega.2c05755
ACS Omega 2023, 8, 614−625

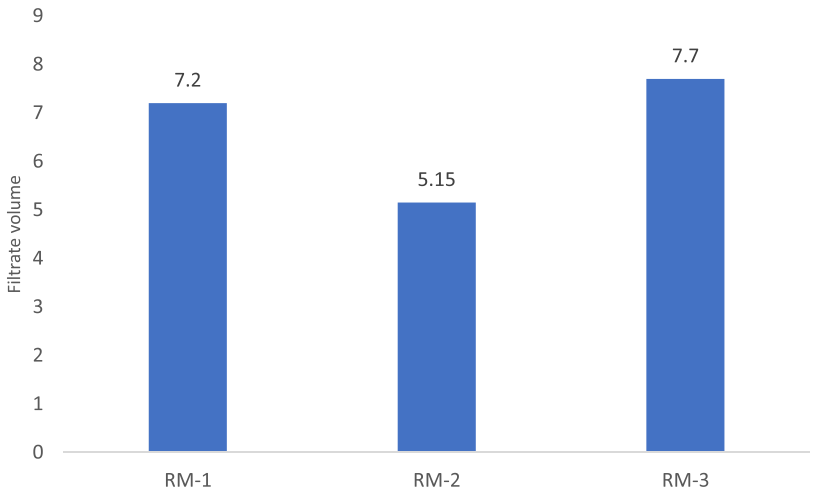

Figure 13. LPLT filtrate (mL).

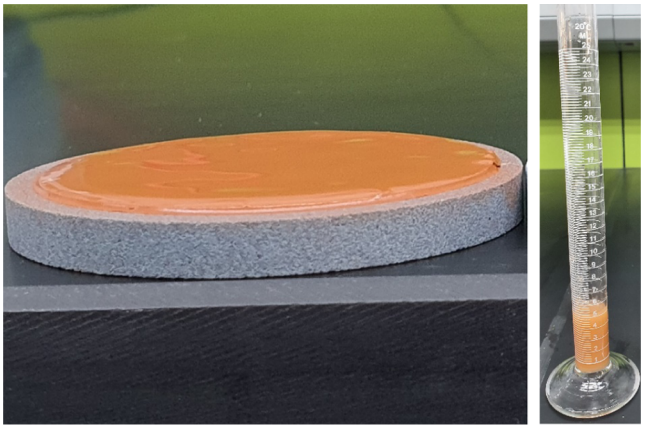

Figure 14. HPHT filter cake and total volume of fluid loss.

(4) The red mud drilling fluid exhibits good filtration performance. The LPLT filtrate for red mud samples ranges from 5.2 to 7.7 mL, and 5.2 mL for the HPHT filtrate, including 2 mL spurt loss.
(5) The treatment process of red mud is comparatively cheap and easy. It only involves drying, grinding, and sieving, which have a minor impact and induce insignificant differences in the rheological behavior.
(6) The red mud additive exhibits good rheological performance and superior filtration behavior. Therefore, the red mud waste could be used as a weighting agent for low-density drilling fluid (LDDF) and as a filtration agent additive in the future.
(7) The data provided in this study for red mud waste provide a reasonable foundation for future comprehensive studies related to red mud waste utilization in

Table 6. HPHT Filtration Testing

@ 150 °F, 250 D.P, 40 μm (μ)	red mud
filter cake thickness, mm	1.50
wet wt [filter cake], gm	11.23
filtrate, mL	5.2

Table 7. Red Mud Acid Dissolution

sample #	sample 1	sample 2	sample 3
testing time	2 h	3 h	4 h
initial weight (g)	2	2	2
residue weight (g) (4 h drying 150 °F)	1.209	1.025	0.93
acid dissolution percentage	39.55	48.75	53.5

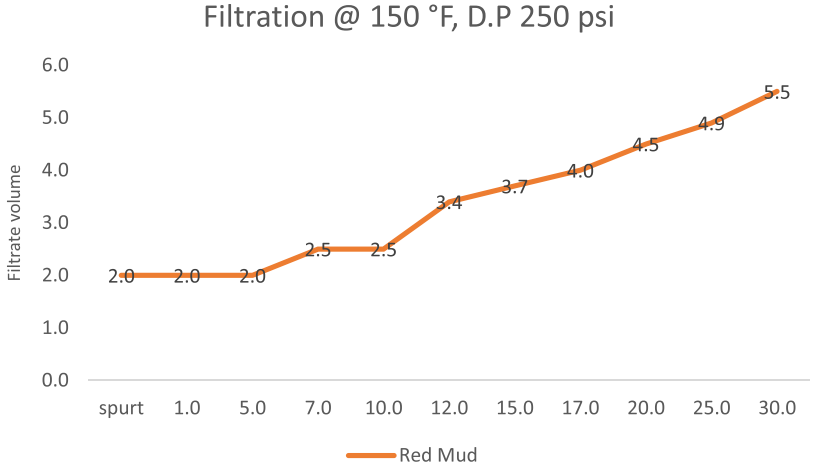

Figure 15. HPHT filtration over 30 min.

https://doi.org/10.1021/acsomega.2c05755
ACS Omega 2023, 8, 614−625

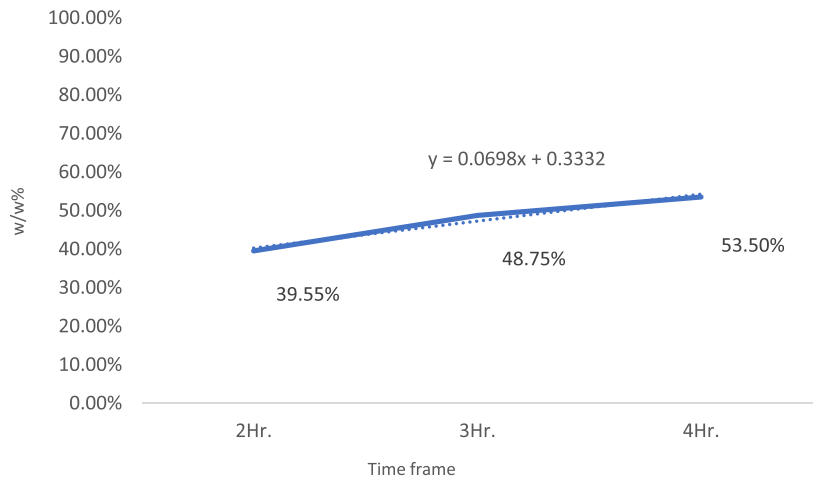

Figure 16. Red mud acid dissolution rate (w/w%) in different time frames.

oil and gas production applications, i.e., drilling and cementing.

AUTHOR INFORMATION

Corresponding Author

Reem AlBoraikan − *College of Petroleum Engineering and Geosciences, King Fahd University of Petroleum & Minerals, Dhahran 31261, Saudi Arabia;* orcid.org/0000-0002-1401-2817; Email: Reem.alboraikan@kfupm.edu.sa

Authors

Badr Bageri − *College of Petroleum Engineering and Geosciences, King Fahd University of Petroleum & Minerals, Dhahran 31261, Saudi Arabia;* orcid.org/0000-0002-7510-0933

Theis I. Solling − *College of Petroleum Engineering and Geosciences, King Fahd University of Petroleum & Minerals, Dhahran 31261, Saudi Arabia;* orcid.org/0000-0003-1710-9072

Complete contact information is available at: https://pubs.acs.org/10.1021/acsomega.2c05755

Notes

The authors declare no competing financial interest.

ACKNOWLEDGMENTS

The authors acknowledge the College of Petroleum Engineering & Geosciences at King Fahd University of Petroleum & Minerals for providing laboratory facilities for conducting this research.

REFERENCES

(1) Wang, S.; Jin, H.; Deng, Y.; Xiao, Y. Comprehensive Utilization Status of Red Mud in China: A Critical Review. *J. Cleaner Prod.* **2021**, *289*, No. 125136.

(2) Agwu, O. E.; Akpabio, J. U. Using Agro-Waste Materials as Possible Filter Loss Control Agents in Drilling Muds: A Review. *J. Pet. Sci. Eng.* **2018**, *163*, 185−198.

(3) Medved, I.; Gaurina-Me, N.; Novak Mavar, K.; Miji′c, P. M. Waste Mandarin Peel as an Eco-Friendly Water-Based Drilling Fluid Additive. *Energies* **2022**, *15*, No. 2591.

(4) Ikram, R.; Jan, B. M.; Sidek, A.; Kenanakis, G. Utilization of Eco-Friendly Waste Generated Nanomaterials in Water-Based Drilling Fluids; State of the Art Review. *Materials* **2021**, *14*, No. 4171.

(5) Murtaza, M.; Tariq, Z.; Zhou, X.; Al-Shehri, D.; Mahmoud, M.; Kamal, M. S. Okra as an Environment-Friendly Fluid Loss Control Additive for Drilling Fluids: Experimental & Modeling Studies. *J. Pet. Sci. Eng.* **2021**, *204*, No. 108743.

(6) Rita, N.; Khalid, I.; Efras, M. R. Drilling Mud Performances Consist of CMC Made by Carton Waste and Na2CO3 for Reducing Lost Circulation. *Mater. Today Proc.* **2021**, *39*, 1099−1102.

(7) Al-saba, M. T.; Amadi, K. W.; Al-Hadramy, K. O.; Al Dushaishi, M. F.; Al-Hameedi, A.; Alkinani, H. In *Experimental Investigation of Bio-Degradable Environmental Friendly Drilling Fluid Additives Generated from Waste*, SPE International Conference and Exhibition on Health, Safety, Security, Environment, and Social Responsibility; OnePetro, 2018, DOI: 10.2118/190655-ms.

(8) Walker, C. O. Alternative Weighting Material. *J. Pet. Technol.* **1983**, *35*, 2158−2164.

(9) Fagundes, F. M.; Santos, N. B. C.; Martins, A. L.; Damasceno, J. J. R.; Arouca, F. O. Gravitational Solid-Liquid Separation of Water-Based Drilling Fluids Weighted with Hematite through the Gamma-Ray Attenuation Technique. *J. Pet. Sci. Eng.* **2019**, *180*, 406−412.

(10) Bageri, B. S.; Gamal, H.; Elkatatny, S.; Patil, S. Effect of Different Weighting Agents on Drilling Fluids and Filter Cake Properties in Sandstone Formations. *ACS Omega* **2021**, *6*, 16176−16186.

(11) Mao, H.; Yang, Y.; Zhang, H.; Zheng, J.; Zhong, Y. Conceptual Design and Methodology for Rheological Control of Water-Based Drilling Fluids in Ultra-High Temperature and Ultra-High Pressure Drilling Applications. *J. Pet. Sci. Eng.* **2020**, *188*, No. 106884.

(12) Al-Bagoury, M.; Steele, C. In *A New, Alternative Weighting Material for Drilling Fluids*; OnePetro; IADC/SPE Drilling Conference and Exhibition, 2012; pp 734−743.

(13) Al-Yami, A. S.; Nasr-El-Din, H. A.; Al-Majed, A. A.; Menouar, H. In *An Innovative Manganese Tetra-Oxide/KCl Water-Based Drill-in Fluids for HT/HP Wells*, SPE Annual Technical Conference and Exhibition; OnePetro, 2007; pp 3380−3407, DOI: 10.2523/110638-ms.

(14) Basfar, S.; Al Jaberi, J.; Elkatatny, S.; Bageri, B. S. Prevention of Hematite Settling Using Perlite in Water-Based Drilling Fluid. *J. Pet. Sci. Eng.* **2021**, *210*, No. 110030.

(15) Samal, S.; Ray, A. K.; Bandopadhyay, A. Proposal for Resources, Utilization and Processes of Red Mud in India — A Review. *Int. J. Miner. Process.* **2013**, *118*, 43−55.

(16) Bageri, B. S.; Benaafi, M.; Mahmoud, M.; Patil, S.; Mohamed, A.; Elkatatny, S. Effect of Arenite, Calcareous, Argillaceous, and Ferruginous Sandstone Cuttings on Filter Cake and Drilling Fluid Properties in Horizontal Wells. *Geofluids* **2019**, *2019*, 1−10.

(17) Bageri, B. S.; Benaafi, M.; Mahmoud, M.; Mohamed, A.; Patil, S.; Elkatatny, S. Effect of Formation Cutting's Mechanical Properties on Drilling Fluid Properties During Drilling Operations. *Arabian J. Sci. Eng.* **2020**, *45*, 7763−7772.

(18) Abdou, M. I.; El-Sayed Ahmed, H. Effect of Particle Size of Bentonite on Rheological Behavior of the Drilling Mud. *Pet. Sci. Technol.* **2011**, *29*, 2220−2233.
(19) Falahati, N.; Routh, A. F.; Chellappah, K. The Effect of Particle Properties and Solids Concentration on the Yield Stress Behaviour of Drilling Fluid Filter Cakes. *Chem. Eng. Sci.: X* **2020**, *7*, No. 100062.
(20) Al Jaber, J.; Bageri, B. S.; Gamal, H.; Elkatatny, S. The Role of Drilled Formation in Filter Cake Properties Utilizing Different Weighting Materials. *ACS Omega* **2021**, *6*, 24039−24050.
(21) Caenn, R.; Darley, H. C. H.; Gray, G. R.*Composition and Properties of Drilling and Completion Fluids*, 7th ed.; Gulf Professional, 2016.
(22) Bageri, B. S.; Adebayo, A. R.; Al Jaberi, J.; Patil, S.; Salin, R. B. Evaluating Drilling Fluid Infiltration in Porous Media − Comparing NMR, Gravimetric, and X-Ray CT Scan Methods. *J. Pet. Sci. Eng.* **2021**, *198*, No. 108242.
(23) Reddy, B. R.; Mishra, S. K.; Banerjee, G. N. Kinetics of Leaching of a Gibbsitic Bauxite with Hydrochloric Acid. *Hydrometallurgy* **1999**, *51*, 131−138.

https://doi.org/10.1021/acsomega.2c05755
ACS Omega 2023, 8, 614−625